



LUND UNIVERSITY

On precoding for overlapped clustering in a measured urban macrocellular environment

Gong, Jie; Zhou, Sheng; Lau, Buon Kiong; Niu, Zhisheng

Published in:

Science in China, Series F: Information Sciences

DOI:

[10.1007/s11432-012-4763-8](https://doi.org/10.1007/s11432-012-4763-8)

2013

Document Version:

Peer reviewed version (aka post-print)

[Link to publication](#)

Citation for published version (APA):

Gong, J., Zhou, S., Lau, B. K., & Niu, Z. (2013). On precoding for overlapped clustering in a measured urban macrocellular environment. *Science in China, Series F: Information Sciences*, 56(2), 022301-38. <https://doi.org/10.1007/s11432-012-4763-8>

Total number of authors:

4

General rights

Unless other specific re-use rights are stated the following general rights apply:

Copyright and moral rights for the publications made accessible in the public portal are retained by the authors and/or other copyright owners and it is a condition of accessing publications that users recognise and abide by the legal requirements associated with these rights.

- Users may download and print one copy of any publication from the public portal for the purpose of private study or research.
- You may not further distribute the material or use it for any profit-making activity or commercial gain
- You may freely distribute the URL identifying the publication in the public portal

Read more about Creative commons licenses: <https://creativecommons.org/licenses/>

Take down policy

If you believe that this document breaches copyright please contact us providing details, and we will remove access to the work immediately and investigate your claim.

LUND UNIVERSITY

PO Box 117
221 00 Lund
+46 46-222 00 00

On Precoding for Overlapped Clustering in a Measured Urban Macrocellular Environment

Gong Jie^{1*}, Zhou Sheng¹, Lau Buon Kiong² & Niu Zhisheng¹

¹*Tsinghua National Laboratory for Information Science and Technology, Tsinghua University,
Beijing 100084, China,*

²*Department of Electrical and Information Technology, Lund University,
Lund 22100, Sweden*

Received July 14, 2012

Abstract In this paper, we study the performance of precoding schemes for cooperative transmission of multiple coherent base stations (BSs) allowing overlapped clustering in a measured urban macrocellular environment at 2.66 GHz to testify the findings obtained by using simulated channel model. The evaluated precoding schemes include zero-forcing (ZF), layered virtual signal-to-interference-plus-noise ratio (SINR) maximization (LVSM) and clustered virtual SINR maximization (CVSM). The results show that the sum rate of the CVSM scheme outperforms the other precoding schemes. In addition, the ZF achieves higher rates than the LVSM, except when the channel condition is poor. When greedy proportional user scheduling is considered, the CVSM scheme and the ZF scheme offer similar performance, whereas the LVSM scheme gives little gain over a non-cooperative transmission scheme used as the baseline.

Keywords Base station cooperation, overlapped clustering, precoding, measured environment, greedy scheduling

1 Introduction

Even though network multiple-input multiple-output (MIMO) technology [1], [2], also known as base station (BS) cooperation or coordinated multi-point (CoMP), has demonstrated great potential of mitigating the interference and enhancing the system capacity, practical implementation of this technology faces the difficulties of acquiring global channel state information (CSI), realizing signal synchronization and so on. Hence, a number of existing studies have instead focused on limited cooperation among a small set of BSs, or namely *BS clustering* [3], [4]. At the same time, achieving the expected large capacity gain requires elaborate designs of wireless resource allocation, including cluster formation, precoding design and scheduling.

In the literature, the BS cluster formation problem has been extensively studied. One popular approach is to form non-overlapping clusters [4]-[7], where each BS is not allowed to belong to different clusters simultaneously. However, there still exist significant number of mobile stations (MSs) at the boundaries of clusters which suffer from strong inter-cluster interference. To address this problem of non-overlapping clusters, recent efforts have considered forming cluster from the viewpoint of the MS, i.e., the best cluster

*Corresponding author (email: gongj08@mails.tsinghua.edu.cn)

of each MS is formed by the BSs with the strongest signals [8]-[10]. As a result, the interference from outside of any given MS's serving cluster, which is called *non-overlapping-BS interference*, is minimized. Nevertheless, this approach may result in some clusters overlapping with each other, causing interference from the overlapped BSs, namely *overlapping-BS interference*.

In this paper, we analyze the performance of the MS-centric clustering approach that allows for overlapped clustering in a real environment. Specifically, we consider three precoding schemes suitable for overlapped clustering. Zero-forcing (ZF) precoding [1] for single-antenna transceiver (or block diagonalization (BD) precoding [6] for multi-antenna case) has been proposed for overlapped clustering in [8], and it aims to fully mitigate the interference. On the other hand, the layered virtual signal-to-interference-plus-noise ratio (SINR) maximization (LVSM) scheme proposed in [11], [12] (also known as signal-to-leakage-plus-noise ratio maximization [13]) maximizes the power ratio between the desired signal of a given MS and the interference to other MSs from each of its serving BSs. As it decides the precoding coefficient of each BS-MS pair individually, the LVSM scheme does not need signal synchronization and can be used for any clustering problem. Finally, the clustered virtual SINR maximization (CVSM) precoding scheme [9], [10] maximizes the virtual SINR from the MS's serving cluster, considering the cluster as "super BS". CVSM is an upgraded version of LVSM.

The main contributions and results we have obtained are listed as follows:

- The coherently measured multi-BS channels of an urban macrocellular environment reported in [14] is adopted for performance evaluation. The measurement setup involves three single-antenna BS and a four-antenna MS traveling along predefined test routes. To the best of our knowledge, this is the first time that the listed schemes are evaluated and compared using the measured channel data from a real environment.
- We analyze the performance of the three precoding schemes without scheduling, i.e., the sum rate of three randomly generated MSs served by the three-BS network. The result shows that the CVSM precoding scheme is the most appropriate precoding technique for overlapped clustering among the three schemes. The performance of the ZF scheme degrades severely in poor channel condition as it reduces to be non-cooperative transmission in such a case.
- We introduce the proportional fair scheduling to evaluate the per-user throughput. The analysis indicates that in our measured environment and with the greedy scheduling policy, the system only schedules the MSs within the same serving cluster. In addition, the ZF and the CVSM precoding schemes facilitate the similar performance for non-overlapped clustering, which verifies the result obtained by using simulated channel.

The rest of the paper is organized as follows. Section 2 introduces the measured urban macrocellular environment, which is used to analyze the performance of the precoding schemes with overlapped clustering. The overlapped clustering setup is described in Section 3. In Section 4, the precoding methods are introduced and evaluated without scheduling. Precoding methods are then evaluated with scheduling in Section 5. Finally, Section 6 concludes the paper.

Notations: $|\cdot|$ denotes the cardinality of a set. $\|\cdot\|$ denotes the Euclidean norm of a vector. $(\cdot)^T$ and $(\cdot)^H$ denote the transpose and transpose conjugate of a matrix or a vector, respectively. \mathbb{C} is the complex number field. \mathbb{E} represents the expectation operation.

2 Measurement Setup

The urban macrocell environment used in the performance evaluation is within Kista, Stockholm, Sweden [14]. A photo of the environment is provided in Fig. 1. The three BS sites that are selected reflect a realistic cellular deployment. Each BS is equipped with a single linearly-polarized antenna mounted above the average rooftop level of around 25 m. Each BS antenna is downtilted by between 6 and 8

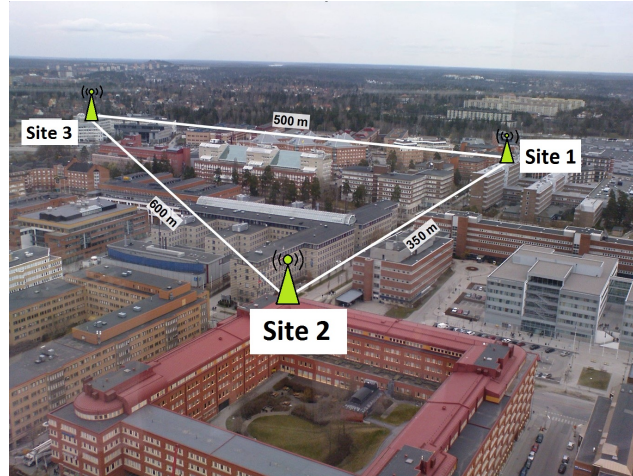


Figure 1: A photograph of measured environment and BS locations.

Table 1: Specifications for the Ericsson Channel Sounder [14]

Parameter	Value
Center Frequency	2.66 GHz
Bandwidth	19.4 MHz
No. of frequency subcarriers	432
Transmit power	36 dBm
Channel acquisition rate	190 channels per second
No. of BS	3
BS antenna	1 (45° polarized antenna)
MS antenna	2 dipole and 2 magnetic loop antennas

degrees from horizontal and the main lobe points towards the centroid of the triangle formed by the three BS sites. On the other hand, the MS is equipped with two dipoles and two loops on the top of a measurement van in a square configuration (with inter-element spacing of around 30 cm).

The channels between all three BSs and four MS antennas are measured using the Ericsson channel sounder described in [14], [15]. RF-over-fiber equipment is used to connect between the transmit unit and the three remote BS sites. Rubidium clocks (Stanford Research Systems, PRS10) are employed at the transmitter and receiver to provide a highly accurate synchronization (Allan standard deviation less than 10^{-12}) between the BS and the MS. The resulting system measures a full 4×3 MIMO channel matrix 1500 times per second (based on 0.667 ms probing frames), but due to practical hardware limitations, only 190 channels are stored per second, which is still sufficient considering the maximum MS speed of 30 km/hr. Relevant parameters for the measurements are given in Table 1 [14].

The measurements involve two different drive routes for the MS (see Fig. 2). The routes include line-of-sight (LOS), obstructed line-of-sight (OLOS), and non-line-of-sight (NLOS) propagation conditions. The geographical location of each channel sample is determined using a GPS receiver.

3 Overlapped BS Clustering

Consider the multiuser downlink cellular system with M cooperative BSs. We study the communication between the BSs and M MSs on a single frequency subcarrier and a single receive antenna. Hence, the

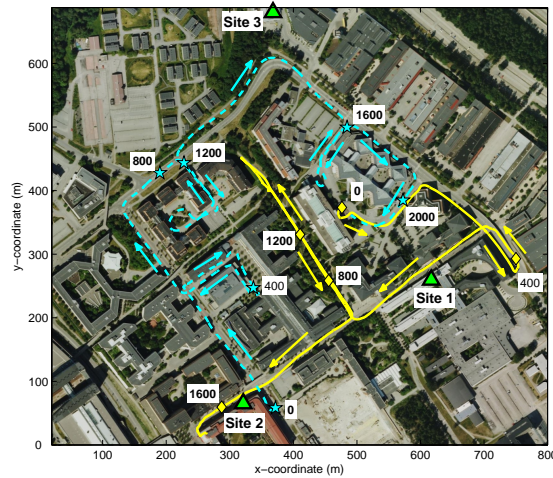


Figure 2: BSs' locations and MS's travel routes 1 (--) and 2 (-). Distances in meters from the starting points are indicated by circles and diamonds for route 1 and 2, respectively. The directions of travel are also indicated.

measured channel can be denoted by a $M \times M$ matrix $\mathbf{H} = \{h_{im}\}_{1 \leq i, m \leq M}$. Assuming limited feedback capability, each MS only feeds back the channel coefficients of the BSs with strongest signals, forming its serving cluster. The serving cluster of MS i is denoted by \mathcal{C}_i , and the cluster size is identical for all the MSs, i.e., $|\mathcal{C}_i| = C$. For simplicity, we assume no synchronization issue among the BSs. The received signal of MS i is given by

$$y_i = \underbrace{\sum_{m \in \mathcal{C}_i} h_{im} w_{im} \sqrt{p_{im}} x_i}_{\text{desired signal}} + \underbrace{\sum_{j \neq i} \sum_{m' \in \mathcal{C}_j} h_{im'} w_{jm'} \sqrt{p_{jm'}} x_j}_{\text{interference}} + n_i, \quad (1)$$

where w_{im} is the normalized precoding coefficient from BS m for MS i , p_{im} is the transmit power, x_i is the desired data signal of MS i , and n_i is the additive white Gaussian noise with zero mean and variance $\mathbb{E}(n_i n_i^H) = \sigma_n^2$. Since only the channel coefficients of MSs' serving clusters are known, the interference can be categorized as overlapping-BS interference (from the BSs $m' \in \mathcal{C}_j \cap \mathcal{C}_i$), which can be effectively mitigated through precoding techniques, and non-overlapping-BS interference (from the BSs $m' \in \mathcal{C}_j \setminus \mathcal{C}_i$). In this sense, we write the received SINR as follows

$$\gamma_i = \frac{\left\| \sum_{m \in \mathcal{C}_i} h_{im} w_{im} \sqrt{p_{im}} \right\|^2}{z_i + \sum_{j \neq i} \left\| \sum_{m' \in \mathcal{C}_j \cap \mathcal{C}_i} h_{im'} w_{jm'} \sqrt{p_{jm'}} \right\|^2}, \quad (2)$$

where $z_i = \sum_{j \neq i} \left\| \sum_{m' \in \mathcal{C}_j \setminus \mathcal{C}_i} h_{im'} w_{jm'} \sqrt{p_{jm'}} \right\|^2 + \sigma^2$ is the non-overlapping-BS interference plus noise power. An example setup of overlapped clustering for cluster size $C = 2$ is depicted in Fig. 3. Given the channel coefficients, the precoding algorithms try to find the proper precoding parameters to maximize the received SINR as in (2).

In our evaluation setup, each BS may serve multiple MSs. Hence, the transmit power of each BS is split for all the served MSs. For simplicity and fairness of comparison, we adopt the *channel aware power splitting* policy proposed in [12], i.e., the power allocation p_{im} is proportional to the channel strength

$$p_{im} = \frac{\|h_{im}\|^2}{\sum_{j: m \in \mathcal{C}_j} \|h_{jm}\|^2} P_0. \quad (3)$$

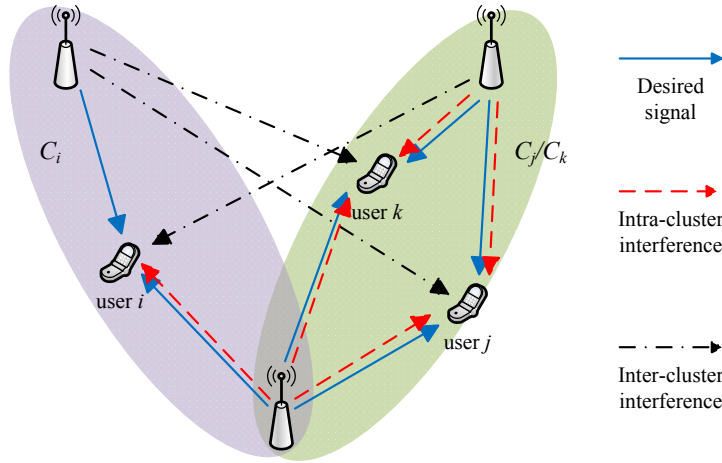


Figure 3: An example setup of overlapped clustering with cluster size $C = 2$.

where P_0 is the BS's transmit power. As a consequence, more power is allocated to the MSs with stronger signal strength to obtain more benefits.

4 Precoding Techniques

In this section, we introduce the principles of the precoding schemes including ZF, LVSM and CVSM, and their specific expressions in our overlapped clustering setup. Then, the performances of these precoding algorithms are compared using measured channels from the urban macrocellular environment.

4.1 Precoding Schemes

4.1.1 ZF

The ZF precoding scheme nulls the interference among the MSs. By mitigating the inter-MS interference, it can achieve high throughput, especially in strong interference scenarios. The ZF precoder is obtained either by the channel inverse $\mathbf{W} = \mathbf{H}^H(\mathbf{H}\mathbf{H}^H)^{-1}$ as stated in [1], or by mitigating the interference from each MS to all other MSs individually. Assume the cluster of MS i is $\mathcal{C}_i = \{m_1^{(i)}, \dots, m_C^{(i)}\}$. The interference channel matrix of cluster \mathcal{C}_i to other MSs is obtained by removing the i th row of \mathbf{H} , and nulling the un-fed back channel coefficients. It is denoted as $\bar{\mathbf{H}}_i = \{h_{jm} I_{m \in \mathcal{C}_j}\}_{j \neq i, m \in \mathcal{C}_i} \in \mathbb{C}^{(M-1) \times C}$, where

$$I_{m \in \mathcal{C}_j} = \begin{cases} 1, & \text{if } m \in \mathcal{C}_j \\ 0, & \text{else} \end{cases} \quad (4)$$

Denote the null space of $\bar{\mathbf{H}}_i$ is \mathbf{V}_i , i.e., $\bar{\mathbf{H}}_i \mathbf{V}_i = \mathbf{0}$. To maximize the desired signal, the precoding vector for MS i is the projection of channel vector between cluster \mathcal{C}_i and MS i on the null space. We calculate

$$[w_{im_1^{(i)}}, \dots, w_{im_C^{(i)}}] = \mathbf{V}_i \mathbf{V}_i^H \bar{\mathbf{h}}_i^H, \quad (5)$$

where

$$\bar{\mathbf{h}}_i = [\sqrt{p_{im_1^{(i)}}} h_{im_1^{(i)}}, \dots, \sqrt{p_{im_C^{(i)}}} h_{im_C^{(i)}}] \quad (6)$$

is the *weighted* channel vector from the cluster \mathcal{C}_i to the user i . Then the precoding vector is then approximated as

$$[w_{im_1^{(i)}}^{\text{ZF}}, \dots, w_{im_C^{(i)}}^{\text{ZF}}]^T \approx \frac{[w_{im_1^{(i)}}, \dots, w_{im_C^{(i)}}]}{\max\{\|w_{im_1^{(i)}}\|, \dots, \|w_{im_C^{(i)}}\|\}}. \quad (7)$$

Note that the power p_{im} might not be fully used, since only the coefficient with the largest $\|w_{im}\|$ is normalized.

To apply the ZF scheme in our specific 3 single-antenna BS environment, a maximum of 3 MSs can be scheduled simultaneously. This is due to limited degree of freedom from the 3 transmit antennas. If the cluster size $C = 3$, the whole network forms a single cluster. Hence, the ZF precoding scheme can be directly used for the scheduled MSs. If the cluster size $C = 2$, as each BS is equipped with one antenna, the interference between 2 MSs in the same cluster can be mitigated. A typical example is as follows. The channel coefficients available at the BSs side are

$$\bar{\mathbf{H}} = \begin{bmatrix} h_{11} & h_{12} & 0 \\ 0 & h_{22} & h_{23} \\ h_{31} & h_{32} & 0 \end{bmatrix}. \quad (8)$$

As MS 1 and MS 3 are in the same cluster, the ZF precoding is applied to them on the subchannel

$$\mathbf{H}_{1,3} = \begin{bmatrix} h_{11} & h_{12} \\ h_{31} & h_{32} \end{bmatrix}, \quad (9)$$

while MS 2 is served only by BS 3. Hence, $w_{22}^{\text{ZF}} = 0$, which means there is not desired signal from BS 2 to MS 2.

In the case that all the MSs have different clusters, the precoding degrades to non-cooperative transmission. The association between MSs and BSs are decided according to the achievable sum rate. For instance, with the channel coefficients available at the BSs side

$$\bar{\mathbf{H}} = \begin{bmatrix} h_{11} & h_{12} & 0 \\ h_{21} & 0 & h_{23} \\ 0 & h_{32} & h_{33} \end{bmatrix}, \quad (10)$$

the precoding scheme degrades to non-cooperative transmission where each MS is served by a single BS with strongest signal strength.

Notice that we assume that for $C = 2$, the case of all the three MSs in the same cluster is prevented by scheduling, since a 2-BS cluster cannot serve 3 MSs simultaneously.

4.1.2 LVSM

As proposed in [12], the LVSM precoding scheme finds the precoding coefficients for each BS by maximizing the ratio between the desired signal of MS i and the interference to other MSs $j \neq i$. It can be expressed as

$$\mathbf{w}_{im}^{\text{LV}} = \arg \max_{\|\mathbf{w}\|^2=1} \frac{\|\mathbf{h}_{im}\mathbf{w}\|^2}{\frac{\sigma_n^2}{p_{im}} + \sum_{j \neq i} \|\mathbf{h}_{jm}\mathbf{w}\|^2}, \quad (11)$$

where \mathbf{h}_{im} represents the MISO channel between the multi-antenna BS m and single-antenna MS i (as opposed to the single-antenna BS assumed earlier). Accordingly, \mathbf{w} is the precoding vector for the MISO transmission. When the single antenna is deployed at each BS and at the MS side, as in this paper, \mathbf{h}_{im} and \mathbf{w} are scalar (rewritten as h_{im} and w respectively), and we have $\|\mathbf{h}_{im}\mathbf{w}\|^2 = \|h_{im}\|^2$. Hence, the right hand side of Eq. (11) is a constant. The optimal precoding coefficient is to keep $h_{im}w$ to be of real value, which means

$$w_{im}^{\text{LV}} = \frac{h_{im}^H}{\|h_{im}\|}. \quad (12)$$

Note that the result is actually equivalent with the maximum ratio transmission (MRT) technique, which tries to maximize the power of the desired signal

$$[w_{im_1}^{\text{MRT}}, \dots, w_{im_C}^{\text{MRT}}]^T = \arg \max_{\|w_{im_1}^{(\theta)}\|=\dots=\|w_{im_C}^{(\theta)}\|=1} \left\| [h_{im_1}^{(\theta)}, \dots, h_{im_C}^{(\theta)}] [\sqrt{p_{im_1}^{(\theta)}} w_{im_1}^{(\theta)}, \dots, \sqrt{p_{im_C}^{(\theta)}} w_{im_C}^{(\theta)}]^T \right\|^2. \quad (13)$$

The closed-form solution of the maximization problem (13) is

$$[w_{im_1}^{\text{MRT}}, \dots, w_{im_C}^{\text{MRT}}]^T = \left[\frac{h_{im_1}^H}{\|h_{im_1}^{(i)}\|}, \dots, \frac{h_{im_C}^H}{\|h_{im_C}^{(i)}\|} \right]^T. \quad (14)$$

Comparing Eq. (12) with Eq. (14), we can easily conclude that the LVSM precoding scheme with single antenna configuration degrades to the MRT precoding scheme, which is optimal in non-interference scenarios. However in our overlapped clustering scenario, the non-managed interference may cause severe performance degradation. Consequently, the LVSM scheme, or the MRT scheme, may not work well.

4.1.3 CVSM

The CVSM precoding scheme [10] is an improved version of the LVSM precoding scheme in order to fully exploit the advantage of clustering. We consider the BSs in each cluster as a ‘‘super BS’’, and design the precoding vector for the super BS which maximizes the ratio between the desired signal of MS i from its serving cluster and the interference of the cluster to other MSs $j \neq i$. Specifically, the optimal precoding vector is calculated as

$$\begin{aligned} [w_{im_1}^{\text{CV}}, \dots, w_{im_C}^{\text{CV}}]^T &= \arg \max_{\|w_{im}\|=1} \frac{\left\| \sum_{m \in \mathcal{C}_i} h_{im} w_{im} \sqrt{p_{im}} \right\|^2}{\sigma^2 + \sum_{j \neq i} \left\| \sum_{m \in \mathcal{C}_i \cap \mathcal{C}_j} h_{jm} w_{im} \sqrt{p_{im}} \right\|^2} \\ &= \arg \max_{\|w_{im}\|=1} \frac{\|\bar{\mathbf{h}}_i \mathbf{w}_i\|^2}{\sigma^2 + \sum_{j \neq i} \|\bar{\mathbf{h}}_{j, \mathcal{C}_i} \mathbf{w}_i\|^2}, \end{aligned} \quad (15)$$

where $\mathbf{w}_i = [w_{im_1}^{(i)}, \dots, w_{im_C}^{(i)}]^T$, $\bar{\mathbf{h}}_i$ is defined in (6), and

$$\bar{\mathbf{h}}_{j, \mathcal{C}_i} = [\sqrt{p_{im_1}^{(i)}} h_{jm_1}^{(i)} I_{m_1^{(i)} \in \mathcal{C}_j}, \dots, \sqrt{p_{im_C}^{(i)}} h_{jm_C}^{(i)} I_{m_C^{(i)} \in \mathcal{C}_j}] \quad (16)$$

is the weighted channel vector from the cluster \mathcal{C}_i to the user $j, j \neq i$, where $I_{m \in \mathcal{C}_j}$ is defined in (4). The per-BS precoding coefficient power constraint in (15) makes the optimal solution difficult to achieve. We achieve the sub-optimal solution by first relaxing the per-BS power constraint to sum-power constraint as

$$[\hat{w}_{im_1}^{(i)}, \dots, \hat{w}_{im_C}^{(i)}]^T = \arg \max_{\|\mathbf{w}_i\|=1} \frac{\|\bar{\mathbf{h}}_i \mathbf{w}_i\|^2}{\sigma^2 + \sum_{j \neq i} \|\bar{\mathbf{h}}_{j, \mathcal{C}_i} \mathbf{w}_i\|^2}. \quad (17)$$

The solution is the unit-norm eigenvector with the largest eigenvalue of $(\sigma^2 \mathbf{I} + \sum_{j \neq i} \bar{\mathbf{h}}_{j, \mathcal{C}_i}^H \bar{\mathbf{h}}_{j, \mathcal{C}_i})^{-1} \bar{\mathbf{h}}_i^H \bar{\mathbf{h}}_i$, where \mathbf{I} is the unit matrix. Then, we get the sub-optimal precoding vector as

$$[w_{im_1}^{\text{CV}}, \dots, w_{im_C}^{\text{CV}}]^T \approx \frac{[\hat{w}_{im_1}^{(i)}, \dots, \hat{w}_{im_C}^{(i)}]^T}{\max\{\|\hat{w}_{im_1}^{(i)}\|, \dots, \|\hat{w}_{im_C}^{(i)}\|\}}. \quad (18)$$

The CVSM precoding scheme provides a good balance between interference minimization and desired signal maximization. Consequently, it is expected to perform well in both high and low interference scenarios, which will be demonstrated in the next subsection.

4.2 Performance Comparison

In this subsection, we compare the performance of the stated precoding methods in the measured urban macrocellular environment. We run the simulation by drops. In each drop, the locations of three MSs are randomly picked from all the measurement points on route 1 and route 2. In fact, it can also be viewed

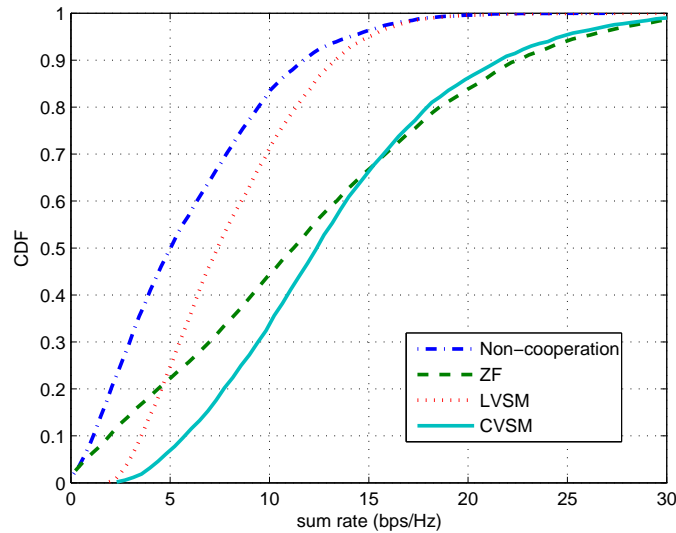


Figure 4: CDF of sum rate with different precoding schemes. The cluster size $C = 2$.

as the round robin scheduling. We assume the each MS uses a single antenna for receiving, i.e., it receives signals only through one of the dipole antennas. We also consider the transmission on a single frequency subcarrier only. Without loss of generality, we select the first one of the 432 frequency subcarriers. As a result, we obtain a 3×3 network MIMO channel matrix. A total of 5000 drops are simulated.

We assume the cluster size is $C = 2$. Each MS only knows the strongest two channel coefficients of BSs, and feeds them back to the network side. The BSs cooperatively design the precoding coefficients for each MS. Once the precoding coefficients are determined, the achievable rate per unit bandwidth of MS i is given by Shannon's capacity formula

$$r_i = \log(1 + \gamma_i) \quad (19)$$

with the unit of bits per second per Hz (bps/Hz), where γ_i is calculated as (2). The evaluation metric considered is the sum rate, which is defined as the sum of the rate of all three MSs.

The cumulative distribution function (CDF) of the sum rate of each drop is depicted in Fig. 4. The baseline is a non-cooperative transmission scheme, by which each MS is served by a single BS with the strongest signal. The result clearly shows that the cooperative transmission scheme outperforms the non-cooperative one. Among different precoding schemes, the CVSM precoding scheme achieves the highest average sum rate, and the performance gain is especially noticeable when the channel condition is poor (take the 10%-outage sum rate as an example, the CVSM scheme is 3.88 times higher than the non-cooperative scheme, 2.06 times higher than the ZF scheme, and 65% higher than the LVSM scheme). The ZF precoding scheme performs well in good channel condition, where the sum rate of ZF scheme is even larger than the CVSM scheme. However, its achievable sum rate is close to the non-cooperative transmission scheme when the channel condition is very poor because it cannot effectively null the interference and thus degrades to single-BS transmission. On the contrary, the LVSM precoding scheme has a higher sum rate in the poor channel condition than the ZF scheme since cooperation enhances the received signal strength. But when the channel condition is good, it brings a much lower performance gain compared with ZF and CVSM schemes, as the interference is not well managed.

5 Joint Clustering and User Scheduling

In this section, we analyze the performance of different precoding schemes for joint overlapped clustering and user scheduling. We assume that a set of MSs \mathcal{U} are randomly generated in the environment. The system selects a subset of MSs \mathcal{S} to be scheduled in each transmission slot depending on the channel conditions of their serving clusters and the average achieved data rate before the current slot. Once the scheduled MSs are determined, they are served according to the precoding schemes presented in Section 4. We adopt the multiuser proportional fair scheduling (MPFS) algorithm [16] to select the MSs. The objective is to maximize the weighted sum rate of all the MSs [10]:

$$\begin{aligned} \max_{\mathcal{S}} \quad & \sum_{i \in \mathcal{S}} \frac{1}{T_i} \log(1 + \gamma_i) \\ \text{s.t.} \quad & \sum_{i: m \in \mathcal{C}_i, i \in \mathcal{S}} p_{im} \|w_{im}\|^2 \leq P_0, \quad m = 1, \dots, M \end{aligned} \quad (20)$$

where T_i is the average throughput of MS i , which is updated slot by slot as $T_i(t+1) = (1 - 1/\tau)T_i(t) + 1/\tau R_i(t)$, where t is the time slot index, τ is the fairness factor [16], and $R_i(t)$ is the instantaneous data rate of MS i in time slot t .

The optimal solution of problem (20) requires an exhaustive search among all possible scheduling subsets, which is NP-hard. We adopt the greedy user selection algorithm based on [17] where MSs are added successively one at a time up to a maximum of M if the weighted throughput is increased. The process is detailed as follows [10]:

1) Find the MS i with the largest weighted rate $\frac{1}{T_i} \log(1 + \gamma_i)$, set $n = 1, \mathcal{S}_1 = \{i\}$.

2) While $n < M$

- Find a MS j^* such that

$$j^* = \arg \max_{j \in \mathcal{U} \setminus \mathcal{S}_n} \sum_{i \in \mathcal{S}_n \cup \{j\}} \frac{1}{T_i} \log(1 + \gamma_i). \quad (21)$$

- If $\sum_{i \in \mathcal{S}_n \cup \{j^*\}} \frac{1}{T_i} \log(1 + \gamma_i) > \sum_{i \in \mathcal{S}_n} \frac{1}{T_i} \log(1 + \gamma_i)$, set $\mathcal{S}_{n+1} = \mathcal{S}_n \cup \{j^*\}$, increase n by 1.

- Else, break.

3) Set $\mathcal{S} = \mathcal{S}_n$.

We simulate the joint scheduling and clustering in the measured environment. We run 100 drops for each precoding scheme. In each drop, a total of 10 MSs are randomly generated and scheduled. The number of scheduling slots in each drop is 100. The channel realizations of each MS during the 100 slots are generated using 50 spatial points within the same shadow fading region (a small region around the chosen MS's location) at two frequencies 20 MHz apart. Fig. 5 shows the CDF of user throughput with different precoding schemes. It can be seen that the ZF precoding scheme and the CVSM precoding scheme have similar CDF curves. On the other hand, the LVSM precoding scheme is slightly better than the non-cooperative scheme, and achieves a little higher user throughput when the cluster size is larger (0.8% average throughput gain of $C = 3$ compared with $C = 2$). The reasons can be found in Fig. 6. It is observed that only one MS is scheduled in each slot with the non-cooperative and the LVSM precoding schemes, which indicates that multiple users scheduled simultaneously will interfere with each other severely. Hence, the measured environment is generally interference-limited. Besides, the number of scheduled MSs and that of transmitting BSs are identical to the cluster size for the ZF and the CVSM precoding schemes, which means that with the greedy algorithm, non-overlapped clusters are scheduled in each slot. Hence, in the measured three-BS environment, non-overlapped clusters are preferred. And with non-overlapped clustering, the ZF and the CVSM precoding schemes are of similar performance, and are better than the LVSM scheme. This verifies the results obtained by using simulated channel model as presented in [10].

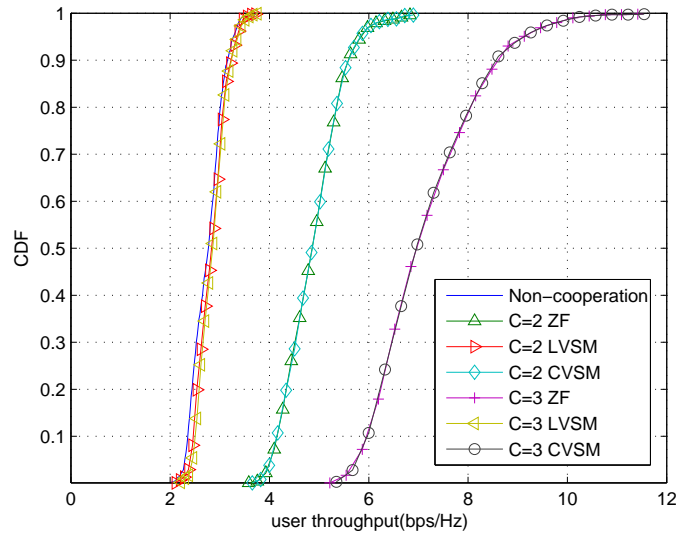


Figure 5: CDF of user throughput with different precoding schemes.

6 Conclusion

In this paper, three precoding schemes for overlapped clustering are evaluated using fully-coherent channel measurements from three BSs to multiple MSs in a macrocellular environment. Without scheduling, the CVSM precoding method is shown to achieve the highest throughput compared with the other two schemes. The ZF precoding scheme is better than the LVSM scheme on average, but is worse in poor channel condition scenario. However, the result is quite different when considering joint clustering and MS scheduling. In this situation, non-overlapped clusters are formed, and the CVSM scheme performs similar with the ZF precoding scheme, while the LVSM scheme introduces slightly higher per-user throughput than the non-cooperative transmission. This is consistent with the simulated results in terms of the performance trends among the precoding schemes. To sum up, CVSM precoding is the best method for the measured environment. Even though the ZF scheme achieves similar per-user throughput as the CVSM scheme with greedy scheduling, further analysis reveals that the latter has better scalability. According to the results obtained using simulated channels in [10], we can predict that the joint overlapped clustering and greedy scheduling will be more useful in larger networks.

Acknowledgements

The authors thank Dr. Jonas Medbo of Ericsson AB, Stockholm for providing the measurement data used in this work. The research work is also sponsored by the International S&T Cooperation Program of China (ISCP) (No. 2008DFA12100); by VINNOVA (No. 2008-00970); by the National Basic Research Program of China (973 Program: No. 2012CB316001); and by the Nature Science Foundation of China (No. 61021001, No. 60925002).

References

- 1 Karakayali M K, Foschini G J, Valenzuela R A. Network coordination for spectrally efficient communications in cellular systems. *IEEE Wireless Commun.*, 2006, 13, 56-61
- 2 Jing S, Tse D N C, Soriaga J B, Hou J, Smee J E, Padovani R. Multicell downlink capacity with coordinated processing. *EURASIP J. Wireless Commun. Netw.*, 2008
- 3 Boccardi F, Huang H. Limited downlink network coordination in cellular networks. *Proc. IEEE Int. Symp. Personal, Indoor, and Mobile Radio Commun. (PIMRC)*, 2007
- 4 Huang H, Trivellato M, Hottinen A, Shafi M, Smith P J, Valenzuela R. Increasing downlink cellular throughput with

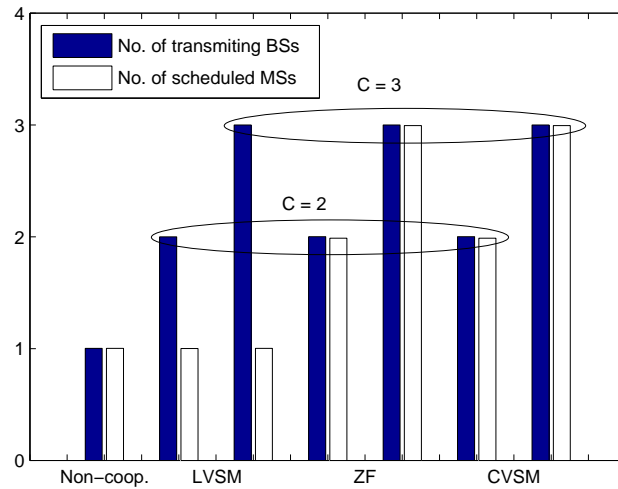


Figure 6: Number of scheduled MSs and transmitting BSs of different precoding schemes.

- limited network MIMO coordination. *IEEE Trans. Wireless Commun.*, 2009, 8, 2983-2989
- 5 Papadogiannis A, Gesbert D, Hardouin E. A dynamic clustering approach in wireless networks with multi-cell cooperative processing. *Proc. IEEE Int. Conference Commun. (ICC)*, 2008
 - 6 Zhang J, Chen R, Andrews J G, Ghosh A, Heath R W Jr. Networked MIMO with clustered linear precoding. *IEEE Trans. Wireless Commun.*, 2009, 8, 1910-1921
 - 7 Zhou S, Gong J, Niu Z, Jia Y, Yang P. A decentralized framework for dynamic downlink base station cooperation. *Proc. IEEE Global Telecomm. Conf. (Globecom)*, 2009
 - 8 Kaviani S, Krzymien W A. Multicell Scheduling in Network MIMO. *Proc. IEEE Global Telecomm. Conf. (Globecom)*, 2010
 - 9 Gong J, Zhou S, Niu Z, Geng L, Zheng M. Joint scheduling and dynamic clustering in downlink cellular networks. *Proc. IEEE Global Telecomm. Conf. (Globecom)*, 2011
 - 10 Gong J, Zhou S, Geng L, Zheng M, Niu Z. A Novel Precoding Scheme for Dynamic Base Station Cooperation with Overlapped Clusters. Accepted by *IEICE trans. commun.* 2012
 - 11 Zakhour R, Gesbert D. Coordination on the MISO interference channel using the virtual SINR framework. *Proc. ITG/IEEE Work-shop Smart Antennas*, 2009
 - 12 Zakhour R, Gesbert D. Distributed multicell-MISO precoding using the layered virtual SINR framework. *IEEE Trans. Wireless Commun.*, 2010, 9, 2444-2448
 - 13 Dai H, Maillander L, Poor H V. CDMA downlink transmission with transmit antenna arrays and power control in multipath fading channels. *European J. Wireless Commun. Networking*, 2004, 1, 32-45.
 - 14 Lau B K, Jensen M A, Medbo J, Furuskog J. Single and multi-user cooperative MIMO in a measured urban macrocellular environment. *IEEE Trans. Antennas Propag.*, 2012, 60, 624-632
 - 15 Selen Y, Asplund, H. 3G LTE simulations using measured MIMO channels. *Proc. IEEE Global Telecomm. Conf. (Globecom)* 2008.
 - 16 Kountouris M, Gesbert D. Memory-based opportunistic multi-user beamforming. *Proc. Int. Symp. Inform. Theory (ISIT)*, 2005
 - 17 Dimic G, Sidiropoulos N D. On downlink beamforming with greedy user selection: performance analysis and a simple new algorithm. *IEEE Trans. Signal Processing*, 2005, 53, 3857-3868